Research Papers

Green and Sustainable MEMBRANES

Green and Sustainable Membranes
Vol. 1, No. 1, June 2026
https://doi.org/10.62755/gsmb.2026.05

Check for updates

Physicochemical Characterization of Graphene Oxide Synthesized from Spent Lithium-Ion Battery Anode Graphite via the Tour Method

Andien Kusumaningtyas[1], Marzuki Naibaho[2,*]

[1] *Department of Chemistry, Faculty of Mathematics and Natural Sciences, Universitas Indonesia, Depok 16424, Indonesia*
[2] *Department of Physics, Faculty of Mathematics and Natural Sciences, Universitas Indonesia, Depok 16424, Indonesia*

Corresponding author: sinaibahomarzuki@gmail.com

ARTICLE HISTORY: Received: March 5, 2026 | Revised: April 10, 2026 | Accepted: April 25, 2026

ABSTRACT

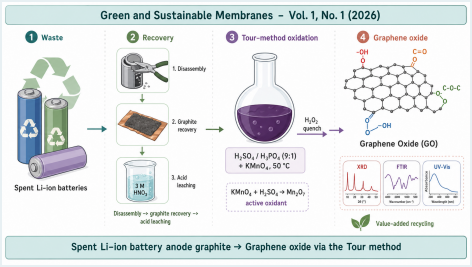

Graphene oxide (GO) was synthesized from graphite recovered from spent lithium-ion battery (SLIB) anodes via the Tour method, and its structural, chemical, and optical properties were investigated. X-ray diffraction revealed broad, low-intensity peaks, indicating a low degree of crystallinity that is consistent with effective oxidation. A prominent (001) reflection at low 2θ confirmed expansion of the interlayer spacing relative to pristine graphite, attributable to the intercalation of oxygen-containing functional groups and trapped water molecules; a residual broad (002) peak indicated partial preservation of graphitic domains with reduced crystallite size. Fourier-transform infrared (FTIR) spectra exhibited absorption bands corresponding to O–H, C=O, C=C, C–O–C, and C–O moieties, confirming the introduction of hydroxyl, carbonyl/carboxyl, epoxy, and alkoxy functionalities. UV–Vis spectra showed a characteristic π–π^* transition near 230 nm associated with sp^2-hybridized aromatic domains, together with a shoulder near 300 nm assigned to n–π^* transitions of carbonyl groups, indicating that the conjugated framework is partially retained alongside the introduced oxygen functionalities. Together, the structural, chemical, and optical signatures confirm that SLIB-derived graphite can be converted into a semi-crystalline GO with abundant oxygen functionalities, supporting the use of waste anode graphite as a feedstock for value-added GO production.

Keywords: *graphene oxide; Tour method; spent lithium-ion battery; anode graphite recycling; oxygen functional groups; UV–Vis spectroscopy*

1. Introduction

Lithium-ion batteries (LIBs) have become the dominant technology in modern energy-storage systems and play a central role in the rapid expansion of electric vehicles and the large-scale integration of renewable energy. The continuously rising global demand for electric vehicles and portable electronics has driven the mass production of LIBs and, in turn, a significant increase in the volume of spent lithium-ion batteries (SLIBs), which is projected to reach millions of tonnes over the coming decades [1–4]. If not properly managed, the accumulation of SLIBs poses serious risks to the environment and to human health [5]. SLIBs contain a wide range of hazardous yet valuable components, including transition metals such as cobalt, nickel, manganese, and iron, as well as non-metallic materials such as carbon and organic electrolyte compounds [6]. The presence of heavy metals and flammable organic electrolytes classifies SLIBs as hazardous waste [7]. At the same time, their high content of valuable materials offers substantial opportunities for sustainable recycling technologies that not only mitigate environmental impacts but also maximize the recovery and reuse of critical resources.

One component that is often overlooked in SLIB recycling is the carbon fraction, which is derived primarily from the graphite used in the anode. Spent anode graphite retains a comparatively stable layered structure and therefore offers strong potential for conversion into high-value carbon materials. Through chemical oxidation, graphite can be transformed into graphene oxide (GO) — a two-dimensional carbon material rich in oxygen-containing functional groups, with a high specific surface area, ease of further functionalization, and good dispersibility in aqueous media [8–11]. Among the available synthesis routes, the Tour method is widely regarded as an effective and reliable approach to GO, as it delivers a high degree of oxidation, enlarged interlayer spacing, and a homogeneous distribution of oxygen-containing functional groups [12,13]. GO obtained via this route exhibits structural and chemical characteristics well suited to applications as electrode materials, functional composites, and supporting components in energy-storage systems and other electrochemical devices. Repurposing spent anode graphite from SLIBs as a precursor for GO synthesis via the Tour method therefore represents a sustainable, high-value-added recycling strategy. Here we report the synthesis and physicochemical characterization (XRD, FTIR, UV–Vis) of GO derived from this waste-graphite feedstock.

2. Experimental Section

2.1 Chemicals and Reagents

Graphite powder was recovered from spent NMC-type lithium-ion battery anodes (see Sections 2.2–2.4). Analytical-grade reagents used for the synthesis were sulfuric acid (H_2SO_4, 97%, Supelco), potassium permanganate ($KMnO_4$,

Supelco), hydrogen peroxide (H_2O_2, 30%, Supelco), hydrochloric acid (HCl, 37%, Supelco), orthophosphoric acid (H_3PO_4, 85%, Supelco), nitric acid (HNO_3, 65%, Merck), and sodium chloride (NaCl). Deionized (DI) water was used throughout.

2.2 Dismantling of Spent Lithium-Ion Batteries

Spent lithium-ion batteries were first immersed in 5 wt% aqueous NaCl for 24 h to ensure complete discharge and to minimize safety risks associated with residual electrical energy. This pretreatment is essential to prevent short circuits, thermal runaway, and accidental ignition during manual handling. The discharged batteries were then dismantled manually: the plastic case was removed with a small knife and the metal casing was opened with cutters and pliers. The cathode, anode, and separator were separated, and only the anode current collector was retained for the subsequent steps.

2.3 Separation of Anode Materials

The anode current collector recovered from the dismantled batteries was cut into approximately 2 × 5 cm pieces and calcined at 120 °C for 3 h. Calcination at this relatively mild temperature was used to remove residual organic binders and other volatile components. The calcined pieces were then immersed in DI water and sonicated for 30 min; sonication weakened the adhesion between the graphite layer and the copper foil, enabling efficient mechanical separation. The graphite was scraped from the copper surface with a spatula, and the recovered copper and graphite fractions were stored separately. The graphite fraction was crushed and sieved through a 400-mesh screen.

2.4 Acid Leaching of the Recovered Graphite

Residual metal contaminants in the recovered graphite were removed by acid leaching using HNO_3. A volume of 180 mL of 3 M HNO_3 was heated to 90 °C, and 6 g of the sieved graphite was slowly added under magnetic stirring. After 1 h, 2 mL of 2% H_2O_2 was added dropwise and the mixture was stirred for a further 10 min. The precipitate was collected and rinsed with 100 mL of distilled water, then dried in an oven at 60 °C for 30 min.

2.5 Synthesis of Graphene Oxide

GO was synthesized from the leached graphite via a modified Tour method. A mixed acid system of concentrated H_2SO_4 and H_3PO_4 (9:1 v/v) was prepared under continuous stirring at room temperature. Graphite (3 g) was added to the acid mixture and stirred for 30 min. $KMnO_4$ was then added gradually at a graphite-to-oxidant mass ratio of 1:6 under continuous stirring. The resulting dispersion was heated to 50 °C and stirred magnetically for 5 h. After the reaction, the purple-brown mixture was poured into a beaker containing ~400 mL of ice-cold DI water and stirred for an additional 1 h, after which 10 mL of H_2O_2 was added, producing a bright-yellow suspension indicative of GO formation. The product was washed with 5% HCl, followed by repeated washing with DI water until the supernatant reached a pH of approximately 3.5–4; each washing step was followed by centrifugation. Probe ultrasonication was then carried out for 5 h until the dispersion turned brown. The dispersion was centrifuged at 10,000 rpm to remove residual impurities, and the recovered material was dried at 50 °C for 24 h, yielding a brown-black GO powder.

2.6 Characterization Techniques

The structural, chemical, and optical features of the synthesized GO were investigated using three complementary techniques. Crystalline structure and interlayer spacing were examined by X-ray diffraction (XRD). Surface functional groups and chemical bonding were probed by Fourier-transform infrared (FTIR) spectroscopy, and optical absorption was recorded by UV–visible spectroscopy over the 200–800 nm range.

3. Results and Discussion

GO was synthesized from the leached SLIB-derived graphite via a modified Tour method, in which strong oxidizing conditions convert graphite into oxygen-functionalized graphene layers. The overall reaction sequence is summarized in Figure 2: $KMnO_4$ reacts with concentrated H_2SO_4 to generate the active oxidant dimanganese heptoxide (Mn_2O_7), which subsequently attacks the graphitic basal planes and installs oxygen-containing functional groups. The mixed H_2SO_4/H_3PO_4 system provides a highly oxidative yet controlled reaction environment that is known to suppress excessive defect formation while promoting uniform oxygen functionalization. Gradual addition of $KMnO_4$ ensures efficient intercalation of Mn_2O_7 between the graphitic layers; at 50 °C the permanganate species oxidize the sp^2 carbon network, installing hydroxyl (–OH), epoxide (C–O–C), and carboxyl (–COOH) functional groups (see Figure 2). These functionalities disrupt π–π stacking, expand the interlayer spacing, and facilitate subsequent exfoliation. Keeping the reaction temperature below 55 °C is essential to avoid over-oxidation and lattice collapse, both of which can result from the spontaneous decomposition of Mn_2O_7 at higher temperatures [14].

Upon quenching the reaction in ice-cold deionized water and adding H_2O_2, a pronounced color change from dark purple-brown to bright yellow was observed. This transformation reflects the reduction of residual $KMnO_4$ to soluble Mn^{2+}, confirming completion of the oxidation step and the formation of graphene oxide sheets. Subsequent washing with dilute HCl effectively removed metal-ion residues, particularly manganese by-products, and repeated centrifugation with DI water progressively raised the suspension pH to 3.5–4. This pH range is characteristic of stable GO dispersions enriched in surface carboxyl groups, which provide electrostatic repulsion and colloidal stability. Finally, extended probe ultrasonication played a decisive role in exfoliating the oxidized graphite into few-layer and single-layer GO sheets.

3.1 XRD Analysis

Figure 3 shows the XRD pattern of the synthesized GO. The pattern exhibits relatively broad, low-intensity diffraction peaks, indicating a low degree of crystallinity that is consistent with effective graphite oxidation. The dominant reflection at low 2θ corresponds to the (001) crystallographic plane and reflects an enlarged interlayer spacing compared with pristine graphite. This expansion is attributed to the intercalation of oxygen-containing functional groups (hydroxyl, epoxide, and carboxyl) and water molecules trapped between the graphene layers. A residual broad feature around the (002) reflection indicates that some graphitic stacking is preserved, albeit with structural distortion and reduced crystallite size as a result of oxidation. Overall, the broadened diffraction features are consistent with the semi-crystalline to amorphous character typical of GO obtained from the Tour method [16].

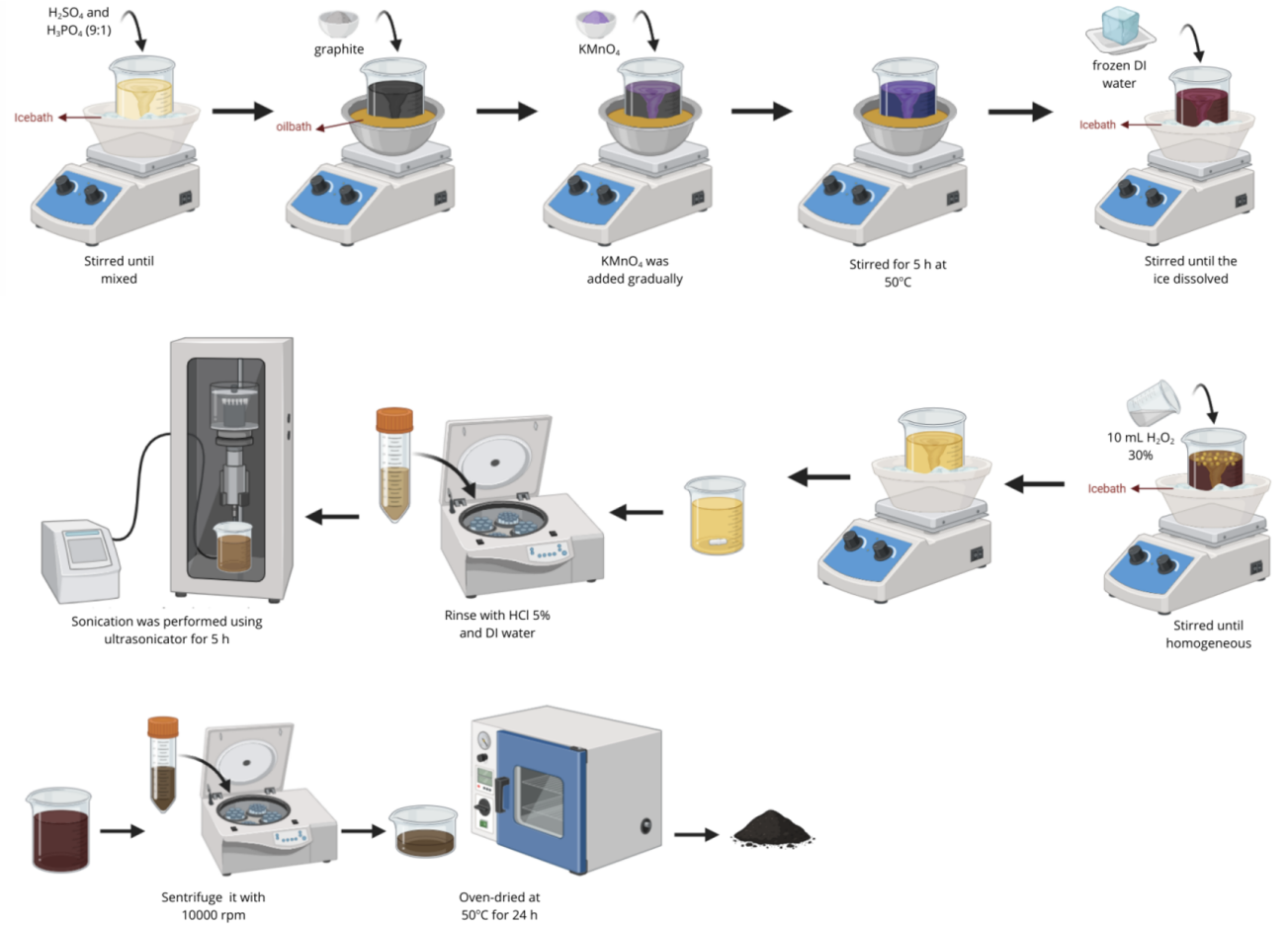

Figure 1. Schematic diagrams of the synthesis processes of GO.

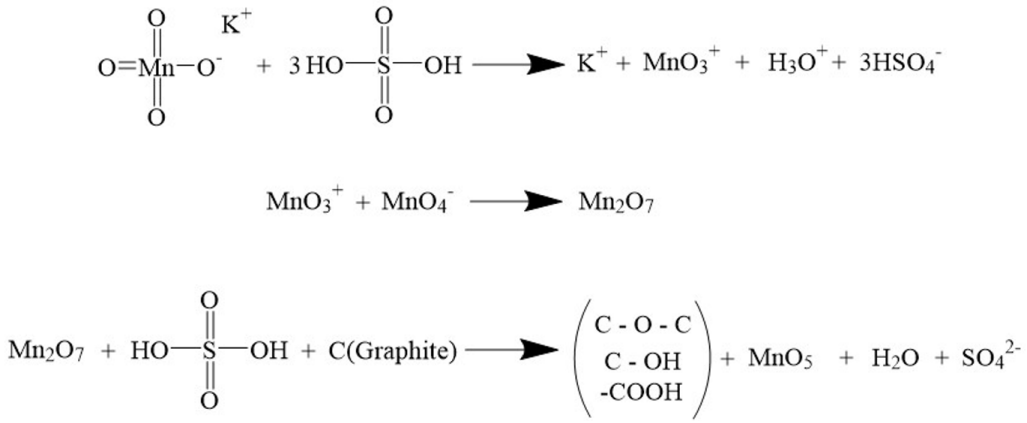

Figure 2. Proposed reaction mechanism for the Tour-method oxidation of graphite to graphene oxide. $KMnO_4$ reacts with concentrated H_2SO_4 to generate the active oxidant dimanganese heptoxide (Mn_2O_7) in situ. Mn_2O_7 then attacks the graphitic basal planes, installing hydroxyl (–OH), epoxide (C–O–C), and carboxyl (–COOH) functional groups while manganese is concomitantly reduced to MnO_3 and soluble Mn^{2+} species.

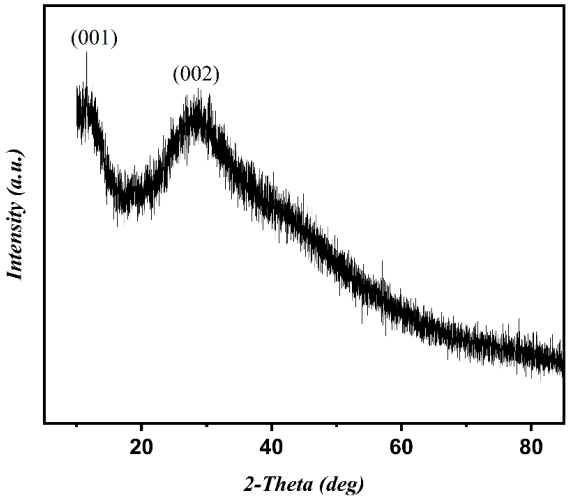

Figure 3. XRD pattern of GO.

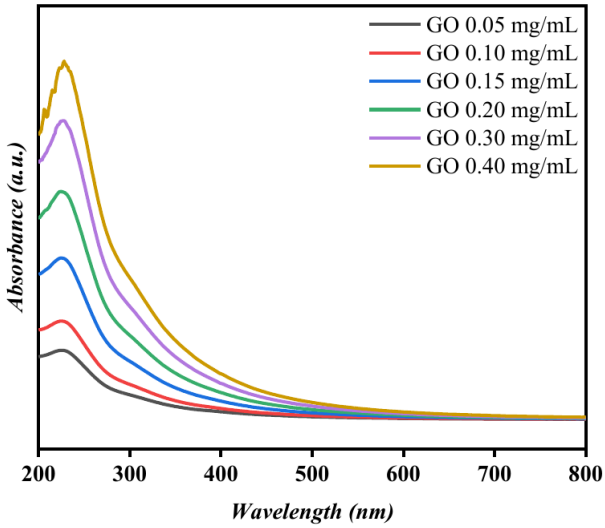

Figure 5. UV–Vis absorption spectra of the synthesized GO recorded at concentrations of 0.05, 0.10, 0.15, 0.20, 0.30, and 0.40 mg mL^{-1}.

3.2 FTIR Analysis

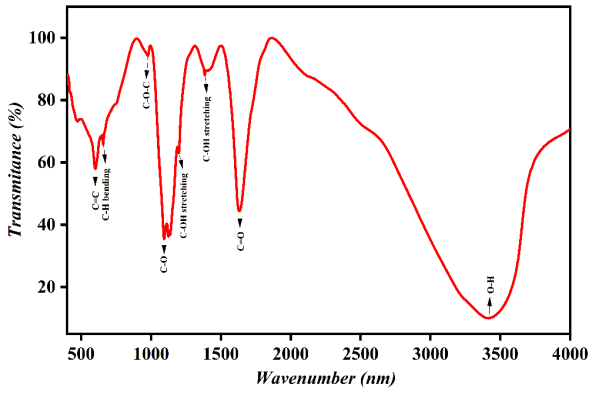

Figure 4. FTIR spectrum of GO.

Figure 4 shows the FTIR spectrum of the synthesized GO, which reveals the suite of oxygen-containing functional groups generated by the oxidation step. A broad absorption between approximately 3300 and 3500 cm^{-1} is assigned to O–H stretching vibrations originating from surface hydroxyl groups and adsorbed water. The peak around 1720–1740 cm^{-1} corresponds to C=O stretching of carboxyl and carbonyl moieties, while the band at 1600–1620 cm^{-1} is attributed to C=C skeletal vibrations of the remaining aromatic graphitic domains. Additional bands at 1220–1250 cm^{-1} and 1030–1100 cm^{-1} are assigned to C–O–C (epoxy) and C–O (alkoxy) stretching vibrations, respectively, which are diagnostic of GO. Together, these signatures confirm a high degree of oxidation and the simultaneous incorporation of hydroxyl, carbonyl/carboxyl, epoxy, and alkoxy groups — features known to enhance the hydrophilicity, chemical reactivity, and interfacial interaction capacity of GO [17,18].

3.3 UV–Vis Analysis

Figure 5 shows the UV–Vis absorption spectra of the synthesized GO at six concentrations between 0.05 and 0.40 mg mL^{-1}. All spectra exhibit a single dominant absorption maximum near 230 nm, accompanied by a weaker shoulder around 300 nm. The 230 nm band is assigned to π–π^* electronic transitions of the aromatic C=C bonds in the residual sp^2-hybridized graphitic domains, while the 300 nm shoulder is attributed to n–π^* transitions of carbonyl groups (C=O), in agreement with the FTIR evidence for –COOH and C=O moieties on the GO surface. These features confirm that the conjugated aromatic framework of the parent graphite is partially preserved alongside the oxygen-containing functionalities introduced by the Tour-method oxidation. Across the concentration series, the absorbance increases monotonically with GO loading without any significant shift in peak position, consistent with a Beer–Lambert response and confirming that the optical signature is intrinsic to the GO sheets rather than to a soluble molecular species. The position of the π–π^* maximum near 230 nm is consistent with values reported for moderately oxidized GO and indicates that the oxidation has not collapsed the conjugated network entirely [15], leaving optical and electronic properties suitable for downstream electrochemical and composite applications.

4. Conclusion

GO was successfully synthesized from spent lithium-ion battery anode graphite via the Tour method, as evidenced by consistent structural, chemical, and optical signatures. XRD confirmed effective graphite oxidation, indicated by a broadened (001) reflection at low 2θ that reflects an enlarged interlayer spacing and reduced crystallinity. FTIR verified the introduction of abundant oxygen-containing functional groups — hydroxyl, carboxyl, carbonyl, epoxide, and alkoxy — which collectively enhance the hydrophilicity and surface reactivity of the product. UV–Vis spectra showed a pronounced π–π^* transition near 230 nm together with an n–π^* shoulder near 300 nm, indicating that the aromatic sp^2 framework is partially preserved alongside the introduced oxygen func-

tionalities and that the optical response scales linearly with GO concentration. These combined structural and electronic features are advantageous for electrochemical and composite applications. Because the carbon fraction of SLIBs is a major recyclable component that is currently underutilized, the successful conversion of waste anode graphite into functional GO highlights a viable pathway for value-added recycling and supports the development of sustainable strategies for lithium-ion battery waste management.

REFERENCES

[1] Chen S, Xiong J, Qiu Y, Zhao Y, Chen S. A bibliometric analysis of lithium-ion batteries in electric vehicles. *Journal of Energy Storage*. 2023;63:107109. doi:10.1016/j.est.2023.107109.

[2] Şen M, Özcan M, Eker YR. A review on the lithium-ion battery problems used in electric vehicles. *Next Sustainability*. 2024;3:100036. doi:10.1016/j.nxsust.2024.100036.

[3] O. Fatoki et al., "Review of Recent Advances in Lithium-Ion Batteries : Sources , Extraction Methods , and Industrial Uses," pp. 1–42, 2025.

[4] P. Parvizi, M. Jalilian, A. M. Amidi, M. R. Zangeneh, and J. Riba, "From Present Innovations to Future Potential : The Promising Journey of Lithium-Ion Batteries," 2025.

[5] Z. Elysia, M. Naibaho, H. Faye, and T. Huang, "The impact of hydrolysis process on the performance of polyacrylonitrile membrane in the separation of dye substances," vol. 9, no. September, 2025.

[6] Zheng X, Zhu Z, Lin X, Zhang Y, He Y, Cao H, Sun Z. A Mini-Review on Metal Recycling from Spent Lithium Ion Batteries. *Engineering*. 2018;4(3):361-370. doi:10.1016/j.eng.2018.05.018.

[7] S. Nowak, Lithium-Ion and Batteries Recycling Edited by.

[8] dan N. I. Fredina Destyorini, Andi Suhandi, Achmad Subhan, "PENGARUH SUHU KARBONISASI TERHADAP STRUKTUR DAN KONDUKTIVITAS LISTRIK," vol. 10, no. 242, pp. 122–132, 2010.

[9] Naibaho M, Fauzi N, Puspita E, Bama AA, Ramlan R, Indayaningsih N. Pembuatan Karbon Serat Sabut Kelapa dan Pengujian Konduktivitas Listriknya. *Jurnal Penelitian Sains*. 2022;24(2):64. doi:10.56064/jps.v24i2.690.

[10] M. Approaches, "Efficient Regeneration of Graphite from Spent Lithium-Ion Batteries through Combination of Thermal and Wet," 2024.

[11] Natarajan S, Mae T, Teah HY, Sakurai H, Noda S. Environmentally friendly regeneration of graphite from spent lithium-ion batteries for sustainable anode material reuse. *Journal of Materials Chemistry A*. 2025;13(7):4984-4993. doi:10.1039/d4ta07618d.

[12] H. Bukovska et al., "Graphite Oxide with High Specific Surface Area," 2023.

[13] Anegbe B, Ifijen IH, Maliki M, Uwidia IE, Aigbodion AI. Graphene oxide synthesis and applications in emerging contaminant removal: a comprehensive review. *Environmental Sciences Europe*. 2024;36(1). doi:10.1186/s12302-023-00814-4.

[14] Emiru TF, Ayele DW. Controlled synthesis, characterization and reduction of graphene oxide: A convenient method for large scale production. *Egyptian Journal of Basic and Applied Sciences*. 2017;4(1):74-79. doi:10.1016/j.ejbas.2016.11.002.

[15] K. S.- Kumar, G. Vázquez, and A. Rodríguez, "Microwave Assisted Synthesis and Characterizations of Decorated Activated Carbon," vol. 7, pp. 5484–5494, 2012.

[16] Huang HH, De Silva KKH, Kumara GRA, Yoshimura M. Structural Evolution of Hydrothermally Derived Reduced Graphene Oxide. *Scientific Reports*. 2018;8(1). doi:10.1038/s41598-018-25194-1.

[17] C. Aguayo and K. Fernández, "Design and Characterization of Chitosan-Graphene Oxide Nanocomposites for the Delivery of Proanthocyanidins," pp. 1229–1238, 2020.

[18] Alves T, Mota WS, Barros C, Almeida D, Komatsu D, Zielinska A, Cardoso JC, Severino P, Souto EB, Chaud MV. Review of scientific literature and standard guidelines for the characterization of graphene-based materials. *Journal of Materials Science*. 2024;59(32):14948-14980. doi:10.1007/s10853-024-10061-4.